
Article:
Marvin, Andrew Charles orcid.org/0000-0003-2590-5335, Ma, Lan, Wen, Yinghong et al. (2 more authors) (2017) A Novel Method for Calculating the Radiated Disturbance from Pantograph Arcing in High-speed Railway. IEEE Transactions on Vehicular Technology. ISSN 0018-9545

https://doi.org/10.1109/TVT.2017.2704611

This article has been accepted for publication in a future issue of this journal, but has not been fully edited. Content may change prior to final publication. Citation information: DOI 10.1109/TVT.2017.2704611, IEEE Transactions on Vehicular Technology

A Novel Method for Calculating the Radiated Disturbance from Pantograph Arcing in High-speed Railway

Lan Ma, *Student Member, IEEE*, Yinghong Wen, *Senior Member, IEEE*, Andy Marvin, *Fellow, IEEE*, Eva Karadimou, Rob Armstrong, Hefei Cao

***Abstract*—Pantograph arcing is a key electromagnetic disturbance source to affect train control system in high-speed railway. Since the characteristics of pantograph arcing is related to train speed, it is necessary to investigate effective numerical modeling and measurement method. However, due to the uncontrollable train speed during on-site measurement, it is difficult to study the radiated disturbance from arcing in the corresponding speed and repeat the same measurement. Therefore, a method combined numerical modeling and reverberation chamber measurements for calculating the radiated disturbance from pantograph arcing in a high-speed railway is proposed. Numerical models of train and sensitive equipment are built to calculate the coupling coefficient in CONCEPT II. And a new measurement procedure in reverberation chamber using pulse signal as the reference source is proposed based on a speed-controllable laboratory replica to measure the total radiated power of pantograph arcing. Then the radiated disturbance from pantograph arcing to the sensitive equipment is achieved with the coupling coefficient and the total radiated power of arcing. The method is verified laboratory experiments. This method can solve the uncontrollable train speed problem during on-site measurement and improve the repeatability of measurement.**

***Index Terms*—pantograph arcing, radiated disturbance, reverberation chamber**

I. INTRODUCTION

THE pantograph is used to collect the current from the power supply by sliding against the lowest catenary contact wire in a high speed railway. However, the separation of the pantograph and the contact wire is unavoidable under some situations, and arcs are generated between the separated gap with consequent broadband radiation. Other studies show that the frequency spectrum of pantograph arcing is from DC to several GHz, which covers the main working frequency of train control system [1]. The electromagnetic field from arcing may interfere the sensitive equipment. In order to study the potential interference from pantograph arcing to communication equipment of train control system, the radiated disturbance characteristics of pantograph arcing should be investigated.

The radiated disturbance from pantograph arcing are usually investigated by two methods: numerical analysis and on-site measurements [2-4]. In [2], a numerical model of pantograph arcing was built in CST to investigate the coupling between the pantograph and antennas on the train roof. The arcing source used in the model was deduced from the signal measured on-site at one position. The simulation can calculate the directivity of arcing and the coupling between antennas. However, pantograph arcing is not omnidirectional antenna and the arcing properties are related to train speed, offline distance, materials of pantograph and catenary, weather and so on which means that single measured field waveform can't represent the real arc. In addition, on-site measurements of pantograph arcing at one position on the train were carried out in [3][4]. The time-domain arcing transients in both AC and DC power supply line (France and Italy) were recorded. Then the rise time, peak amplitude and time duration of received transients in different conditions were statistically analyzed. However, since the electromagnetic characteristics of arcing are affected by the train speed which is not easy to control, on-site measurement is time consuming and difficult to repeat.

To study electromagnetic characteristics of pantograph arcing in a controllable environment, experiments with pantograph arcing setup are taken in laboratory. A setup to generate arcing with a section of real catenary and a full-size pantograph could be found in [5]. The pantograph arcing in a static train is generated by raising and lowering the pantograph. To study the arcing phenomena during train running, an improved pantograph arcing setup was proposed by S. Midya team [6-8]. The conducted emission of pantograph arcing in both DC and AC traction power supply was investigated in detail in their experiments. However, there is a lack of investigation on the radiated characteristics. Based on above discussion, an efficient method needs to be investigated to study the radiated disturbance from pantograph arcing.

In this paper, a novel method which combines numerical modeling and laboratory experiments is proposed. By analyzing

This work was supported in part by the China Railway Project (2016J011-H). (Corresponding author: Yinghong Wen)

Lan Ma, Yinghong Wen and Hefei Cao are with the Electromagnetic Compatibility Laboratory, School of Electronic and Information Engineering, Beijing Jiaotong University, Beijing, 100044 China and Beijing Engineering Research Center of EMC and GNSS Technology for Rail Transportation, Beijing 100044 China (e-mail: lan20557418@hotmail.com, yhwen@bjtu.edu.cn, hfcao@bjtu.edu.cn).

Andy Marvin is with the Department of Electronic Engineering, University of York, York YO10 5DD, U.K. and York EMC Services Ltd, York YO10 5DD, U.K. (e-mail: andy.marvin@york.ac.uk)

Eva Karadimou and Rob Armstrong are with York EMC Services Ltd, York YO10 5DD, U.K. (e-mail: eva.karadimou@yorkemc.co.uk, rob.armstrong@yorkemc.co.uk)

This article has been accepted for publication in a future issue of this journal, but has not been fully edited. Content may change prior to final publication. Citation information: DOI 10.1109/TVT.2017.2704611, IEEE Transactions on Vehicular Technology

the coupling between pantograph arcing and communication equipment of train control system, the radiated disturbances from pantograph arcing are calculated. In this method, the radiated disturbance from pantograph arcing to a system is assessed by the coupling power. Firstly, numerical models of pantograph arcing and the communication equipment are built in CONCEPT II to calculate the coupling coefficient between them. And the variability of the coupling coefficient under four different conditions (inclined arcing, zigzag structure of contact wire, oscillation of contact wire or train and folding pantograph) is also discussed. Secondly, based on a speed-controllable pantograph arcing replica, a new measurement procedure using pulse signal as the reference source to measure the total radiated power of pantograph arcing in reverberation chamber is proposed and verified by a comparison of several experiments. At last, the coupling power is calculated with the coupling coefficient and the total radiated power.

The organization of this paper is as follows. In Section II, the numerical simulation models of pantograph arcing and communication equipment are built to calculate the coupling coefficient under different conditions. The pantograph arcing replica and the measurement procedure of the total radiated power are presented in details in Section III. Section IV shows the results and discussions of the calculated coupling power and the electric field along the railway. The application scope and the limitation of this method are also given in this section. The conclusions are stated in Section V.

II. COUPLING COEFFICIENT BETWEEN ARCING AND SENSITIVE EQUIPMENT

Nowadays the information used for train control system are transmitted by the GSM-R antenna (uplink: 876 - 880MHz, downlink: 921 - 925MHz) on the train roof. As the analysis in Section I, the pantograph arcing may interfere the GSM-R communication system. Signal-to-noise ratio is an important criterion for evaluating whether a communication system is interfered [9]. It is calculated by the ratio of signal power and noise power. For the communication system, the radiated disturbance from pantograph arcing is noise. Thus the coupling power, which is the noise power received by GSM-R antenna, is important for evaluating the disturbance level. To explain the proposed method clearly, the calculation of the coupling power from pantograph arcing to GSM-R antenna on a typical train is illustrated as an example in the following sections. And to achieve the coupling power, the coupling coefficient is calculated first by numerical models of train and GSM-R antenna in CONCEPT II.

A. The Coupling Coefficient of Pantograph Arcing and GSM-R Antenna

The coupling coefficient in this paper is a ratio of the voltage on the arc source and the voltage coupled to the GSM-R antenna. It can be computed by numerical models in Concept-II program[10], which uses an Integral Equation Boundary Element simulation solved by the Method of Moments in the frequency domain. A model of a typical train with the pantograph and GSM-R antenna on the same carriage is shown in Fig. 1. However, considering the GSM-R frequency, the train carriage is an electrically-large object which is a challenge to the computer memory and the calculation time. For the coupling coefficient between the arcing and GSM-R antenna, the train roof and the catenary are the important components of the model. Therefore, the model is simplified with only important components as shown in Fig. 2: the train roof, the pantograph, the contact wire, the GSM-R antenna and the arc between the pantograph and the contact wire. In addition, two ports are built at the arc feeding point and the GSM-R feeding point. The coupling coefficient is presented by the |S21| (or |S12|) between the two ports in the program.

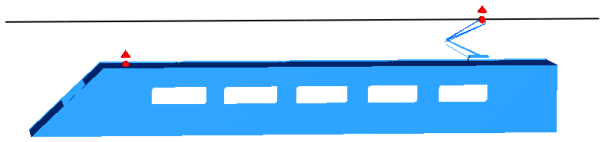

Fig. 1. A typical model of train with pantograph and GSM-R antenna

Fig. 2. A simplified model for the coupling coefficient of pantograph arcing and GSM-R antenna

Arc discharge is an electrical breakdown of a gas between two electrodes. The ionized channel of arc is usually treated as a cylinder structure, such as the classical Cassie[11] and Mayr[12] arc models. Therefore, the arc is modelled as a short wire, and works as the excitation segment of the whole structure including pantograph, contact wire and train roof. In the model, these structures are conducted and produce radiation as a whole radiator. The main radiated parts are within a sphere with about a wavelength (about 0.33m for 900MHz) radius around the arc. The arc length is built as 30mm in the initial model. The GSM-R antenna is simulated as a quarter-wavelength monopole working at 900MHz. For a typical model of train, the size and shape of the carriage and the pantograph are both known. In this model, the size of train roof is set in 19m×2.82m. A single-arm pantograph which is widely used in the railway is built in the model. The length of contact wire is infinite compared to the carriage length in railway and the limited length built in the model may affect the coupling coefficient significantly. Thus, the simplified structure needs to be justified by the length of contact wire.

In order to investigate the influence of contact wire length, the contact wire is built as different lengths in a series of models. The lengths extending from arc and GSM-R antenna positions to the nearby terminals are kept the same (L1 = L2 in Fig. 2). An ideal ground is built instead of the train roof to accelerate the calculation speed. By comparing 110 models which the total contact wire length is increased with 0.2m steps from 21m to 43m (66 wavelengths), a trend of sine waveform with unequal amplitudes can be clearly observed on all the S-parameters between the feeding ports in Fig. 3 (a). It is difficult to determine the coupling coefficient according to these values.

To reduce the variation scope of S-parameters in different contact wire lengths, loads are added on the contact wire at a

This article has been accepted for publication in a future issue of this journal, but has not been fully edited. Content may change prior to final publication. Citation information: DOI 10.1109/TVT.2017.2704611, IEEE Transactions on Vehicular Technology

quarter-wavelength to both terminals. Considering the catenary and the train roof as a pair of "transmission lines", the impedance is mismatched at the open end. The reflections on the contact wire make the field around the contact wire sensitive to the length. Thus the coupling coefficient varies with different contact wire lengths. However, for the open end transmission line, the impedance looking from a quarter–wavelength to the open end is zero. Therefore, adding loads between the contact wire and the train roof could be simulated by adding loads at a quarter-wavelength to the contact wire terminals to absorb the oscillation energy. 50Ω and 200Ω resistors are used in 110 models, respectively. The S-parameters simulated by models with 200Ω loads are shown in Fig. 3 (b). To investigate the effect of catenary loads, a comparison is made by the model with no load, 50 Ω load and 200 Ω load on the contact wire. The results show that the variation scope of coupling coefficient is clearly reduced with larger resistor (from 28dB with no load to 4dB with 200 Ω load), while the average values almost keep the same (the maximum difference is only 1.3dB). Therefore, the variation of the coupling coefficient caused by the length of contact wire can be solved by adding loads on two terminals. With larger resistors, the coupling coefficient is closer to the average value.

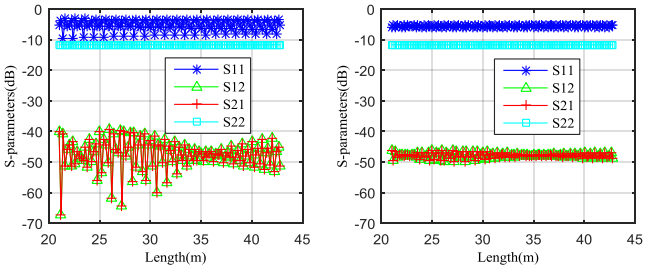

(a) No load on the catenary (b) 200Ω loads at a quarter-wavelength to the catenary terminals

Fig. 3. S-parameters (port 1: Arcing feeding point; port 2: GSM-R feeding point) for catenary length between 21m and 43m in ideal ground model without train roof

Based on above analysis, the basic model to achieve the coupling coefficient between pantograph arcing and GSM-R antenna is comprised by the contact wire with 200Ω loads at two terminals, the train roof, the single-arm pantograph, the arc and GSM-R antenna. The coupling coefficient is achieved by averaging the |S21| calculated from a series of such basic models including different contact wire lengths changing in several wavelengths. More accurate results can be obtained by changing a smaller step of the contact wire length in the models, and adding more models. In this paper, 100 models are built with the contact wire changing from 21m to 31m (30 wavelengths). The S-parameters of the above models are shown in Fig. 4 and the average values are summarized in TABLE 1. The coupling coefficient (|S21|) is -44.88dB between pantograph arcing and GSM-R antenna.

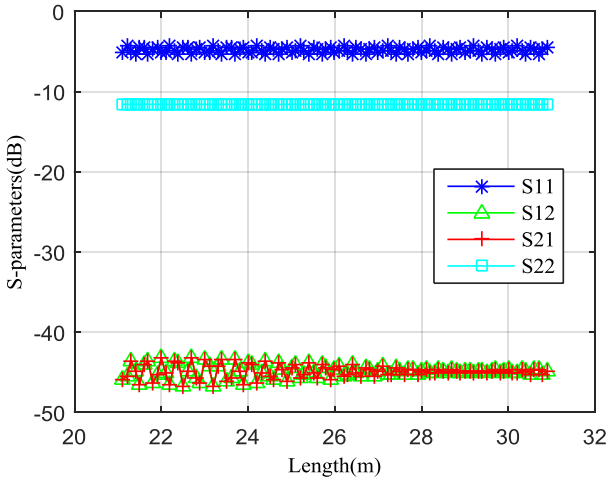

Fig. 4. S-parameters (port 1: Arcing feeding point; port 2: GSM-R feeding point) for basic model (catenary length between 21m and 31m)

TABLE I
THE AVERAGE VALUE OF S-PARAMETERS FOR BASIC MODELS

	|S11|	|S12|	|S21|	|S22|
Average(dB)	-4.83	-44.88	-44.88	-11.60

B. Verification of the Coupling Coefficient by Scale Model

To verify the correctness of the above coupling coefficient computed by numerical models, a scale model of pantograph arcing and GSM-R antenna is designed to measure the coupling coefficient (S21) between them. Based on similitude theory, when the physical dimensions of the model antenna are M times smaller than the real antenna, and the measured frequency and conductivity are M times larger than the real antenna, the electromagnetic field will be the same in the model antenna and the real antenna, where M is the scaling factor[13]. 10 is used as the scaling factor for the full-size pantograph arcing and GSM-R antenna shown in Fig.2, which means that measurements made with the scale model at a frequency of 9GHz will represent the performance of the coupling in the real structure measured at a frequency of 900MHz.

The scale model is shown in Fig.5. The physical dimensions of train roof, pantograph, contact wire and GSM-R are all 10 times smaller than the real structure. Due to the high conductive materials used in the real antenna, it is difficult to find materials which conductivities are 10 times higher. Therefore, in practice, materials with high conductivities are usually utilized in the scale model. The train roof uses aluminum alloy plate, and other parts adopt high conductivity copper wires to simulate. The measurement frequency is 9GHz. To reduce the influence of contact wire length, 200Ω loads are added in the contact wire at a quarter-wavelength to the terminals. Due to the limitation of experimental conditions, the scale model ignores the influence of the cross-section area of pantograph, and the wire radiuses of contact wire and GSM-R antenna. The gap between pantograph and contact wire is Port 1, and the feeding port of GSM-R antenna is Port 2. A network analyzer is used to measure the S-parameters between the two ports. To avoid the interference

This article has been accepted for publication in a future issue of this journal, but has not been fully edited. Content may change prior to final publication. Citation information: DOI 10.1109/TVT.2017.2704611, IEEE Transactions on Vehicular Technology

from the field radiated and received by cables, shield cables are used in measurement. When the GSM-R antenna is disconnected, the S21 measured is -79dB, which further proves that the cables will not affect the coupling coefficient measurement.

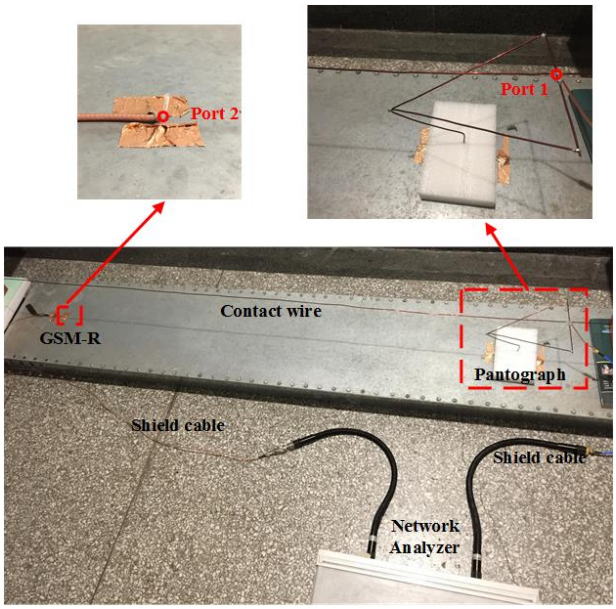

Fig.5. Scale model

The measurement result shows that the S21 between the two ports in the scale model is -47dB at 9GHz, which means the coupling coefficient between pantograph arcing and GSM-R antenna in the real structure is -47dB at 900MHz. Comparing with the simulation result, there is 2.12dB difference which is acceptable. The error may come from neglecting the influence of the wire radiuses in the scale model. Therefore, the coupling coefficient calculated by numerical models is proved to be valid by the scale model.

C. The Variability of the Coupling Coefficient

During the train running, the structure of arc may change in some situations, resulting in a variation of the coupling coefficient.

Firstly, the arc initiates in the vertical direction and as the train moves it starts getting inclined. This situation can be observed by the replicas made in laboratory[5,14]. The inclined arc changes the length and directivity of "arc antenna" which may affect the coupling coefficient. Therefore, the inclined arcing is the first situation need to be considered.

Secondly, in railway, the layout of contact wire is zigzag in horizontal plane to reduce the wear of pantograph. Parts of the pantograph and the contact wire constitute the main radiated parts of "antenna" together with arc. This zigzag contact wire changes the "antenna" structure and it is unavoidable. It is necessary to investigate the influence of zigzag structure of contact wire to the coupling coefficient.

The above two situations are unavoidable when the train runs. There are also a lot of external factors may influence the "arc antenna" conditions sometime, such as ice layer in winter, the poor quality of contact wire, the uneven railway and so on. In this paper, three changes in physical structure are considered at last: contact wire oscillates, train oscillates and pantograph folds during the train running. To the "arc antenna", the first two oscillations result in the same changes. Thus this is considered as the third situation. And pantograph folding is the last situation considered in the paper.

The above four situations may occur at the same time during the train running. As research, the four situation are considered separately in this paper. The details are shown as follows:

1) Inclined arcing

The arcs in previous models are simulated by a segment in vertical direction. In real conditions, the arc is inclined between the contact wire and the pantograph while the train is running. The arc root on the contact wire always changes while the arc root on the pantograph almost keeps at the same position. With the current ionized arc root on the contact wire, the impedance of arc is smaller than the arc made by a new root in a new place on the contact wire for some distance. This arc root will maintain until the arc impedance become larger than the arc with new root on the contact wire. Therefore, when the train is running, the arc roots on the contact wire and pantograph can't keep the same speed at first. The arc root on the contact wire lags a little than the root on the pantograph, which results in the inclining arc. The variability of coupling coefficient caused by the inclined arc is considered in the model shown in Fig. 2. And the inclined arc part is detailed in Fig. 6. The vertical distance between the contact wire and the pantograph is assumed as a constant (30mm) in the model. The arc is built by an inclined dipole which the length increases from 30mm to 90mm. The variability of the coupling coefficient caused by the inclined arcing is -48.80dB to -44.90dB as shown in Fig. 7. The coupling coefficient shown in the figure is calculated by averaging |S21| from a series of models with different contact wire lengths as presented in Section II, Part A.

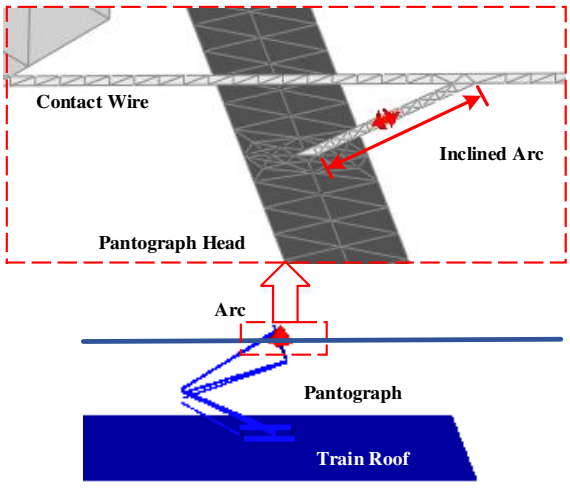

Fig. 6. The inclined arc

This article has been accepted for publication in a future issue of this journal, but has not been fully edited. Content may change prior to final publication. Citation information: DOI 10.1109/TVT.2017.2704611, IEEE Transactions on Vehicular Technology

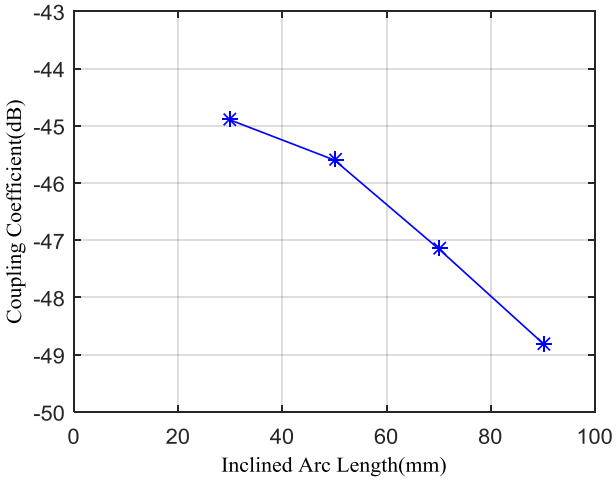

Fig. 7. The coupling coefficient with the inclined arc

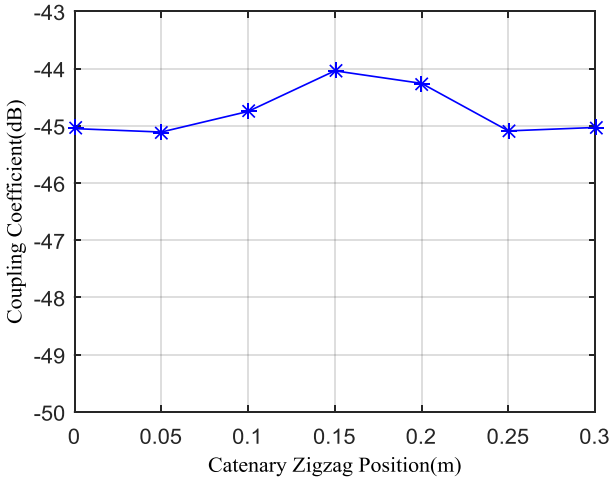

Fig. 9. The coupling coefficient with the zigzag contact wire

2) Zigzag structure of contact wire

To reduce the wear of the pantograph, the contact wire is made in zigzag structure in horizontal plane as shown in Fig. 8. The contact point of the contact wire and the pantograph changes between *a* and *b* on the pantograph head. With the zigzag contact wire, seven series of models are built to simulate the variability of coupling coefficient caused by this situation. The distance between adjacent anchor points is 40-60m; the horizontal distance from the middle of pantograph to the anchor points is ±300mm. Therefore, the zigzag angle α of contact wire to the driving direction is 0.86°. The arc keeps the same length (30mm) and different positions on the pantograph: in the middle, 0.05m, 0.1m, 0.15m, 0.2m, 0.25m, 0.3m on one side of pantograph. The variabilityof the coupling coefficient caused by the zigzag structure is -45.20dB to -44.10dB as shown in Fig. 9.

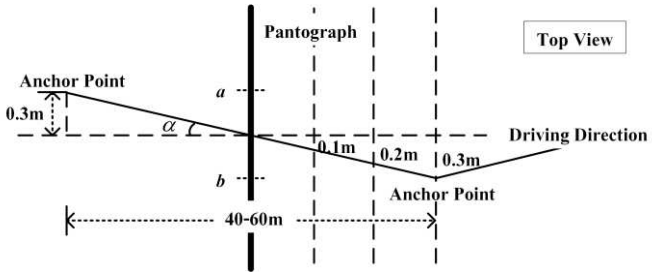

Fig. 8. The zigzag structure of contact wire

3) Contact wire or train oscillates along the railway

Due to the complicated geography and the limitation of technical quality, the rail and the contact wire are uneven at some places, resulting in the oscillation of the contact wire or the train while the train is running. In this situation, the height between the catenary and the train roof varies, which leads to the variation of the gap between the pantograph and contact wire when they separate. This situation results in the changes of arc length by adjusting the contact wire height in the basic model. To simulate this case, 5 series of models with arc length increasing from 10mm to 90mm are respectively built corresponding to the increasing of contact wire height.

Fig.10 shows the trend of coupling coefficient changing with arc length. The variability of the coupling coefficient caused by the oscillation of catenary and train is -49.89dB to -43.72dB.

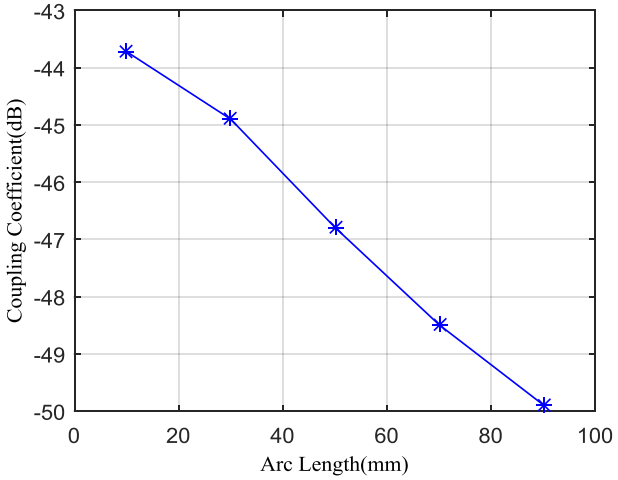

Fig. 10. The coupling coefficient with the oscillation of catenary or train

4) Pantograph folds while train running

When the train is running stably and the contact wire keeps straight along the railway, the height between the contact wire and train roof maintains a constant value. However, the pantograph may oscillate which also results in a change of the arc length and then affect the coupling coefficient. The single-arm pantograph structure is shown in Fig. 11. The angle

This article has been accepted for publication in a future issue of this journal, but has not been fully edited. Content may change prior to final publication. Citation information: DOI 10.1109/TVT.2017.2704611, IEEE Transactions on Vehicular Technology

between the upper arm and lower one may have a little change when the train is running. This situation is simulated in our models by adjusting the pantograph angle. Thus the arc length changes from 10mm to 90mm corresponding to the different pantograph angle. Five series of models are built for this structure. The calculation method of coupling coefficient is the same with the first situation. The variability of the coupling coefficient caused by the folding pantograph is -49.64dB to -43.66dB as shown in Fig. 12.

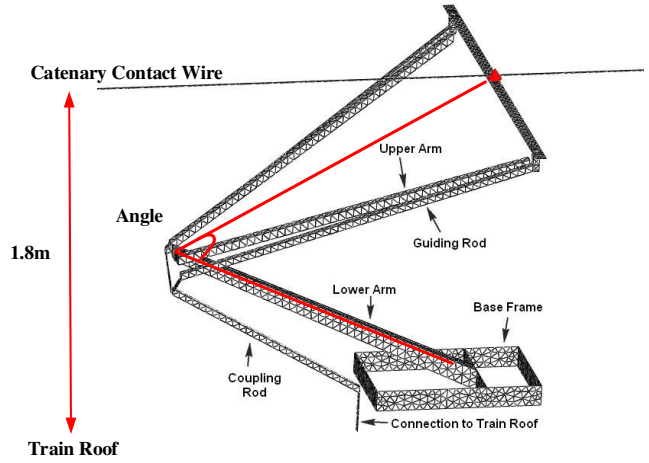

Fig. 11. The arc length changes by the varying angle of pantograph

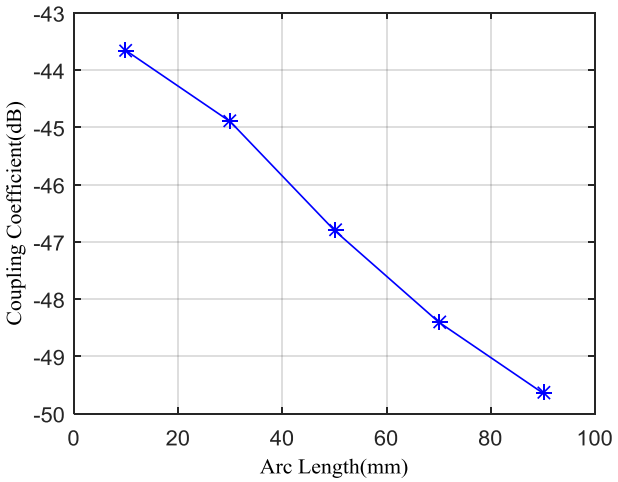

Fig. 12. The coupling coefficient with the oscillation of pantograph

Comparing the four situations, the variability caused by the zigzag structure is much smaller. The main parameter to affect the coupling coefficient is the arc length. Considering all the situations, the variability of the coupling coefficient between the pantograph arcing and the GSM-R antenna is -49.89dB to -43.66dB.

III. THE TOTAL RADIATED POWER OF PANTOGRAPH ARCING

With a mobile train, the radiation properties of an arcing pantograph can be observed and measured on site but not in a controlled and easily quantifiable way. In an anechoic chamber, it's also a challenge for the scanning system that the directivity of arc source is difficult to predict. Therefore, the total radiated power of pantograph arcing is proposed to be measured in a reverberation chamber. To investigate and present the measurement method, a speed-controllable laboratory replica of pantograph arcing has been constructed to simulate the arcing phenomena in high-speed railway.

A. The Laboratory Replica of Pantograph Arcing

The laboratory replica is designed to be operated easily and safely in a reverberation chamber. In this case, the chamber size is 4.70m×3.00m×2.37m. The structure of the replica is designed in CONCEPT II and is verified to represent the real pantograph arcing with the same arcing source to investigate the radiated power [11].

The photograph of the designed laboratory replica is shown in Fig. 13. A rotating wheel is used in the replica to simulate the very long contact wire and a metal rod is employed as the pantograph. The high supply voltage is generated by an automotive ignition system and a circuit is designed to control the ignition system to offer about 40kV DC voltage at a rate of 100 times per second. The mechanism of arcing generation in this replica is the same with pantograph arcing in high-speed railway environment. When the supply voltage is higher than the breakdown voltage of the gap between the pantograph and the contact wire, arcing will be generated. Based on the above design, the replica can generate 100 arcs per second to represent the arcing in 50Hz AC traction system.

In this replica, the pantograph keeps still and the contact wire moves in a circle. Thus the speed of the train can be replicated by the speed of the wheel edge according to the relative movement. The rotation of wheel is controlled by a DC motor connected to the axle. In the demonstration model the train speed can be adjusted from 0 to 35km/h by controlling the current of the motor and monitored by a speed meter.

All modules in the replica are supplied by 12V DC batteries separately which have no high frequency radiation. The rotation of wheel and arcing can be switched on and off outside of the chamber using a shield cable through the wall.

In order to test the emission all come from the arcing, two experiment have been done to the motor and arc igniter which may also produce radiated disturbance except pantograph arcing. The DC motor used in this replica is 321-3192 which has an electric brush inside. One experiment is only turn on the DC motor in the replica and measure the emission; the other is change the gap between pantograph and wheel long enough to make the voltage between them can't generate the arc, thus the emission measured are all come from the arc igniter. There is no emission captured by spectrum analyzer at 900MHz in both experiment. Thus it is proved that the emission of the replica are all coming from the arcing.

This article has been accepted for publication in a future issue of this journal, but has not been fully edited. Content may change prior to final publication. Citation information: DOI 10.1109/TVT.2017.2704611, IEEE Transactions on Vehicular Technology

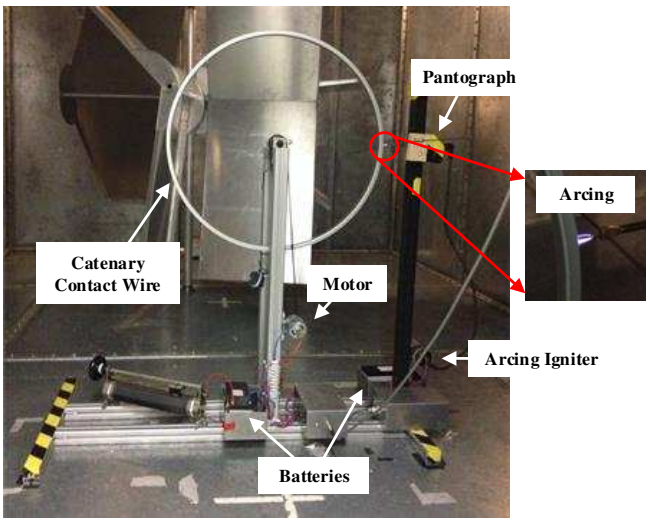

Fig. 13. The laboratory replica of pantograph arcing

Fig. 14 shows the arc signals generated by the replica at 900MHz in time-domain in the reverberation chamber at one stirrer position. It is captured by a Spectrum Analyzer setting at 900MHz frequency and zero span in 1s sweep time. The frequency of arc occurrence is 100Hz which is the same as designed above.

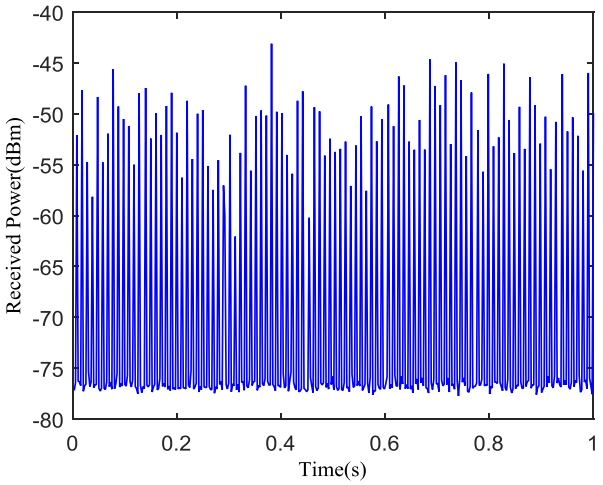

Fig. 14. The arc signal captured in the reverberation chamber in time-domain

This replica is a simple arcing pantograph model which can be operated in the chamber. Though it couldn't represent the exactly same arc in railway, this replica is enough to investigate and present the measurement method. The replica will be more accurate with a real pantograph head, a piece of real contact wire on the edge of wheel, a larger wheel and an AC power supply.

B. Measurement Method of the Total Radiated Power of Arcing in Reverberation Chamber

Based on the linear property of the reverberation chamber, a known power source is used as a reference to calculate the total radiated power of an equipment under test. Generally, the reference source and the radiation signal from the equipment should be wider than 2.5 times of the chamber time constant (typically defined as 10μs [15]) to reach the stable field response in the chamber for accurate results. Therefore, the time constant of our chamber should be measured first to make sure whether the current measurement method is suitable for the arcing signals.

1) Q-factor and time constant of the reverberation chamber

The chamber Q-factor determines the sensitivity of the chamber in emission measurements. In other words, with higher Q-factor, the smaller intensity of emission will be measured but a longer time is needed to reach the stable field response. In our case, a shorter time constant is required to measure the short arcing pulses. Several absorber block (AN79) are added to the chamber one by one in order to reduce the time constant.

The laboratory replica is put inside the chamber with the power off as the ambient while measuring the Q-factor and the time constant,

$$Q = \frac{16\pi^2 V}{\lambda^3} \cdot \frac{\langle P_R \rangle}{\langle P_T \rangle} \tag{3}$$

$$\tau = \frac{Q}{2\pi f} \tag{4}$$

where Q is the Q-factor, τ is the time constant, V is the chamber volume, λ is the wavelength and f is the frequency, P_T is the power transmitted into the chamber by the reference antenna and P_R is the power received by the receive antenna, <>is the average value over all the stirrer positions during one complete rotation.

The measurement results are shown in TABLE II.

TABLE II
Q-FACTOR AND TIME CONSTANT OF THE REVERBERATION CHAMBER

No. Absorbers	Q	τ	2.5τ
0	4327	0.76μs	1.9μs
1	1772	0.31μs	0.78μs
2	1225	0.22μs	0.54μs
3	790	0.14μs	0.35μs
4	653	0.12μs	0.29μs

According to TABLE II, the time constant measured in the chamber with 4 absorbers loaded is still longer than the width of arc pulse captured in the open field (about 0.05μs). No more absorbers can be added because the Q-factor is too small to catch the arc signal.

In this case, the arc signal is much shorter than the 2.5 times time constant. It means that the arc response in the chamber can't reach the stable state before the arc vanishes. The usual reference source – a continue wave signal of a known power which can always get to the stable state in the chamber is not suitable for the pantograph arcing measurement. A new measurement method of the radiated power of pulse signal is necessary to be investigated.

2) Measurement method

According to the characteristic of the arc signal, a measurement method of the total radiated power, for periodic unmodulated pulse signals with pulse width less than 2.5 times of the chamber time constant, is investigated by experiments in the reverberation chamber. It can be used to measure the total

This article has been accepted for publication in a future issue of this journal, but has not been fully edited. Content may change prior to final publication. Citation information: DOI 10.1109/TVT.2017.2704611, IEEE Transactions on Vehicular Technology

radiated power of pantograph arcing without considering the directivity of arcing. A periodic unmodulated pulse signal (similar to pantograph arcing) is considered as the reference source. The total radiated power of arcing is calculated by comparison to this reference source. The proposed procedure of the measurement is shown as follows:

a) The power of the reference pulse signal

The reference pulse signal is generated by a Pulse Generator. The total radiated power of the pulse is measured directly by connecting to a Spectrum Analyzer. Since the concerned frequency is only 900MHz, a band-pass filter is added before the spectrum analyzer to protect it as shown in Fig. 15. The power measured in this way is the total radiated power of the reference pulse at a single frequency. It is measured at 900MHz center frequency, zero span and different Resolution Bandwidths (RBW) of the spectrum analyzer, as P_{TXcal}. $\langle P_{TXcal} \rangle$ is the average results of 100 pulse power without the noise floor.

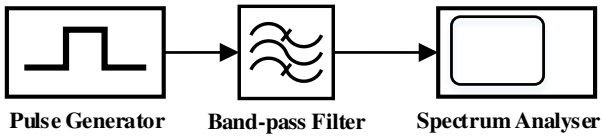

Fig. 15. The measurement of pulse power into the reference antenna

b) The received power from the reference antenna

The configuration of the measurement is shown in Fig. 16. During this measurement, the pantograph arcing replica is put in the chamber with power off as an ambient. The power is provided by the signal generator and received by the spectrum analyzer through antennas. The received power is recorded for 1s at 1 stirrer position, and 100 stirrer positions are utilized in 1 stirrer revolution. The spectrum analyzer is set at 900MHz with zero span. An RF filter is used before the spectrum analyzer, the same with the measurement of the reference pulse signal power. For the power recorded on the spectrum analyzer at 1 stirrer position, the noise floor is removed first and the received power P_{RXcal} is recorded by averaging the value of all the pulses caught during 1s. $\langle P_{RXcal} \rangle$ is the average value of P_{RXcal} in all stirrer positions in 1 stirrer revolution.

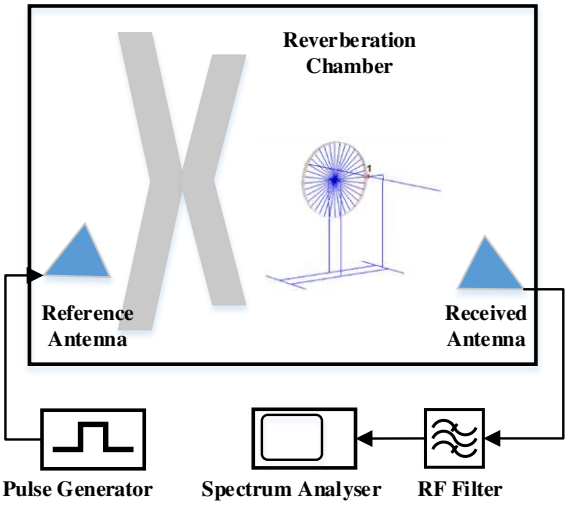

Fig. 16. The measurement configuration of power received from the reference pulse signal

c) The received power from pantograph arcing

To keep the same Q-factor of the chamber, the reference antenna can't remove when measuring the received power from pantograph arcing. To protect the pulse generator, a 50Ω load is added instead of the pulse generator in Fig. 16 to keep the same input impedance of the reference antenna. The replica works continuous in 1 revolution of the stirrer. The received power $\langle P_{RXARC} \rangle$ is the average values over 100 stirrer positions with noise floor removed.

d) The total radiated power of pantograph arcing replica

The total radiated power of arcing can be calculated by (5):

$$P_{ARC} = \langle P_{RXARC} \rangle \cdot \frac{\langle P_{TXcal} \rangle}{\langle P_{RXcal} \rangle} \tag{5}$$

3) The verification of the measurement method

This measurement method is verified by two methods respectively. One is comparing a known pulse power to the results calculated by this measurement method. The measurements utilize different types of pulses as the reference source to enhance the verification; the other is measuring the same radiated power of the known pulse signal in different reverberation chambers. This is simulated by adding absorbers into the same chamber to change the Q-factor instead.

In both verifications, the known pulse (width=1ns, rise and fall time=0.3ns, amplitude=3.6V, periodicity=0.01s) generated by the pulse generator is assumed as the equipment under test (EUT). The real radiated power of this pulse can be measured by the method in Fig. 15. The results are presented in different RBW in TABLE III. RBW could be seen as the bandwidth of the receiver. For narrowband signals, which the bandwidth of the signal is smaller than the RBW on the spectrum analyzer, the received power doesn't change with different RBW. But for broadband signal, such as pulses, which the spectrum is much wider than the largest RBW, the received power on the spectrum analyzer highly depends on the setting of RBW. With the larger RBW of the 'sensitive equipment', the wider spectrum are involved thus the larger radiated power can be received. The measurement results in both verifications are used to compare to real total radiated power in TABLE III. If they are the same or in a tolerable difference, the new measurement technique can be verified as good.

TABLE III
THE REAL TOTAL RADIATED POWER OF PULSE EUT

RBW	100kHz	300kHz	1MHz	3MHz
Power (dBm)	-65.54	-56.23	-47.75	-40.37

a) Different reference pulses

The main parameters for unmodulated pulse signal include the pulse width, amplitude, rise time, fall time and periodicity. The periodicity of pulse in all measurements is set as 0.01s which is the same with 100 arcs in 1s. The amplitude for reference source doesn't matter because the ratio in (5) is used. Thus two series of measurements with different pulse widths and rise (fall) times are set for the verification respectively. The settings of all reference pulses are shown in TABLE IV.

This article has been accepted for publication in a future issue of this journal, but has not been fully edited. Content may change prior to final publication. Citation information: DOI 10.1109/TVT.2017.2704611, IEEE Transactions on Vehicular Technology

TABLE IV
REFERENCE PULSE SETTINGS

No.	Pulse	Width	Rise time	Amplitude	Period
1	EUT	1ns	0.3ns	3.6V	10ms
2	Reference	10ns	0.25ns	5.0V	10ms
3	Reference	10ns	0.5ns	5.0V	10ms
4	Reference	500ns	0.25ns	5.0V	10ms
5	Reference	500ns	0.5ns	5.0V	10ms
6	Reference	3μs	0.25ns	5.0V	10ms
7	Reference	3μs	0.5ns	5.0V	10ms
8	Reference	1μs	0.3ns	5.0V	10ms
9	Reference	3μs	0.3ns	5.0V	10ms

The measurement procedure introduced in last section is taken for each measurement. The radiated power of the assumed pulse EUT is calculated by different reference pulses in TABLE IV(No.2~No.7) respectively. The results sorted by rise time are shown in Fig. 17. The black wire with the triangle mark is the real radiated power of the pulse EUT in TABLE III. Fig. 18 is the same data but sorted by different pulse widths. In both Fig. 17 and Fig. 18, the radiated powers measured in different pulse references are all around the real value in 3dB error. This error may be caused by the weak reference pulse. The power measured by the spectrum analyzer is the sum of input power and noise floor. When the received reference power is close to the noise floor, the ratio of $<P_{TXcal}>$ and $<P_{RXcal}>$ is not accurate.

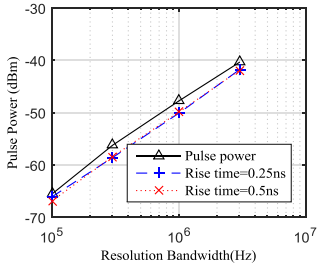

(a) Reference Pulse Width=10ns

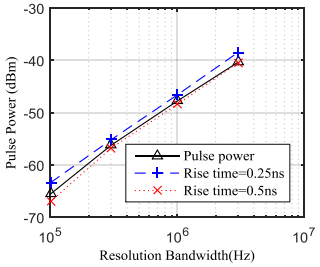

(b) Reference Pulse Width=500ns

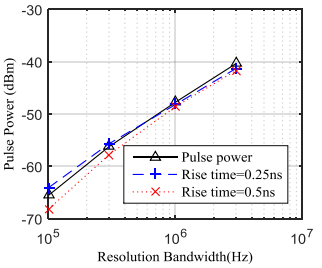

(c) Reference Pulse Width=3μs

Fig. 17. The radiated power of pulse measured in different rise times

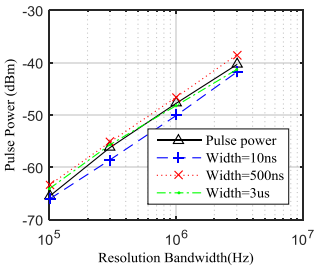

(a) Reference Pulse Rise Time = 0.25ns

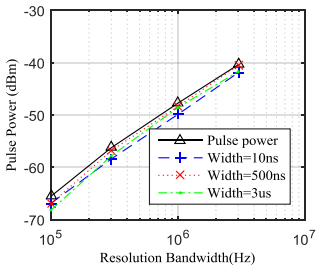

(b) Reference Pulse Rise Time = 0.5ns

Fig. 18. The radiated power measured in different pulse widths

b) Different reverberation chambers – Change Q-factor

The different reverberation chambers are simulated by adding different numbers of absorbers into the same chamber. This can change the Q-factor of the chamber in order to simulate different reverberation chambers. In this validation, the reference pulse is set as No.8 and No.9 in TABLE IV. Four pieces of AN79 absorbers are added into the chamber one by one. The measurement procedure is the same with *a)*. According to the results shown in Fig. 19, the measured radiated powers agree well with the real radiated power in less loading, especially in higher RBW. This suggests the measurement for pulse radiated power is better performed in high-Q chamber. It is not necessary to reduce the Q-factor to achieve longer time constant.

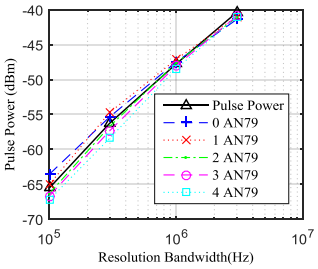

(a) Reference Pulse Width=1μs

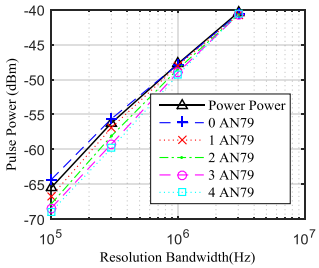

(b) Reference Pulse Width=3μs

Fig. 19. The radiated power measured in different Q-factors of the chamber

Based on the above two verifications, the measured radiated powers all agree with the real power of the pulse EUT within 3dB. And the verification shows that the pulse measurement is better to process in a high Q-factor reverberation chamber, not long time constant. In conclusion, the measurement method is valid for pulse signal, which can be used for the pantograph arcing measurements.

C. The Total Radiated Power of the Arcing Pantograph Replica

With the measurement method investigated in Section III, part B, the total radiated power of pantograph arcing under different train speeds can be measured with the laboratory replica. In initial measurement, the train speed is set as 0, and the gap between the wheel and the pantograph is 5mm. To get more accurate results, 3 reference pulses (No.1~No.3 in TABLE IV) are chosen to calculate the radiated power of arc. The results are shown in Fig. 20.

This article has been accepted for publication in a future issue of this journal, but has not been fully edited. Content may change prior to final publication. Citation information: DOI 10.1109/TVT.2017.2704611, IEEE Transactions on Vehicular Technology

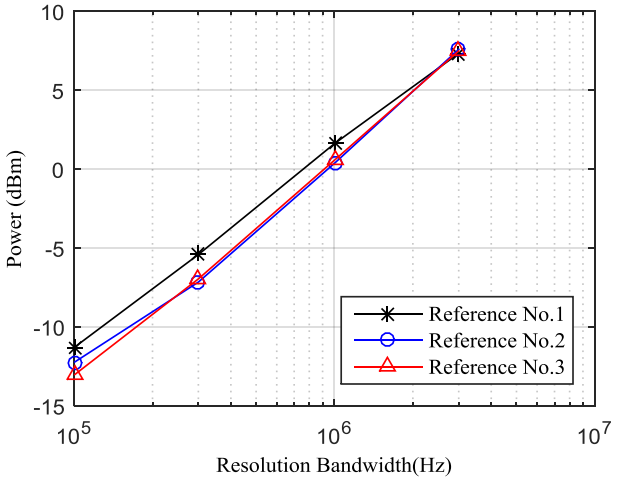

Fig. 20. The total radiated power of pantograph arcing replica

The average value of the power measured by 3 reference pulses in each RBW is shown in TABLE V. This is the total radiated power of pantograph arcing produced by the laboratory replica.

TABLE V
THE TOTAL RADIATED POWER OF PANTOGRAPH ARCING REPLICA

RBW	100kHz	300kHz	1MHz	3MHz
Power (dBm)	-12.20	-6.51	0.85	7.47

IV. THE RADIATED DISTURBANCE FROM PANTOGRAPH ARCING TO GSM-R ANTENNA

A. *The Calculation of the Coupled Power*

According to the numerical models in section II, the coupling coefficient between pantograph arcing and GSM-R antenna $(|S21|)_{dB}$ is -49.89dB to -43.66dB. The total radiated power from the pantograph arcing replica measured in reverberation chamber (P_{ARC}) is shown in TABLE V in different RBW. Therefore, the power coupled to GSM-R antenna P_{Couple} can be calculated by:

$$P_{Couple} = P_{ARC} \cdot \left(|S21|\right)^2 \tag{6}$$

The equation calculated in dB is:

$$\left(P_{Couple}\right)_{dBm} = \left(P_{ARC}\right)_{dBm} + \left(|S21|\right)_{dB} \tag{7}$$

The coupled power from pantograph arcing to GSM-R antenna calculated by (7) is shown in TABLE VI.

TABLE VI
THE COUPLED POWER FROM PANTOGRAPH ARCING TO GSM-R ANTENNA

RBW	100kHz	300kHz	1MHz	3MHz
Min-Coupled Power (dBm)	-62.09	-56.40	-49.04	-42.42
Max-Coupled Power (dBm)	-55.86	-50.17	-42.81	-36.19

The bandwidth of GSM-R channel is 200kHz. Limiting by the setting on the spectrum analyzer, the RBW can't set at 200kHz. To predict the maximum disturbance, the coupled power in 300kHz RBW is chosen as the value close to reality. Thus the radiated disturbance from pantograph arcing coupled to GSM-R antenna is -56.40dBm to -50.17dBm.

B. *The Calculation of E-field along the Railway*

The E-field distribution can be achieved from the numerical model. Fig. 21 shows the E-field on the plane 0.1m height above the train roof. The input power of arc is 1W sine signal at 900MHz. With the total radiated power measured in Section III, the real E-field can be calculated at any position concerned by the following calculation.

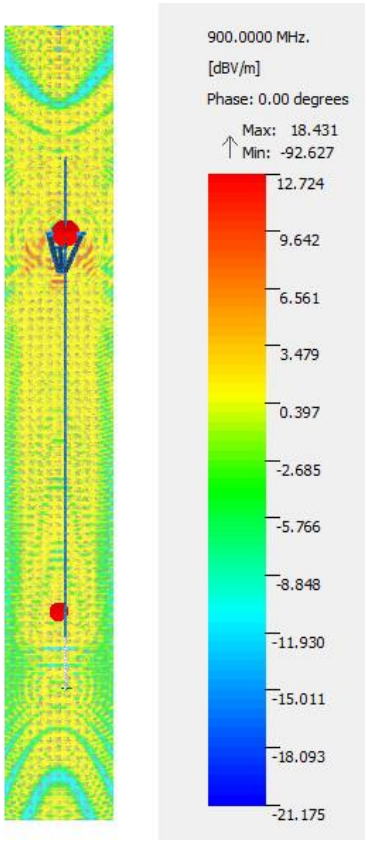

Fig. 21. The E-field on the plane above the train roof 0.1m height with 1W arc power

Define the input power of arc as P_{in} and the power transmits from the "arc antenna" as P_t. Thus

$$P_t = P_{in} \cdot \left(1 - |S11|^2\right) \tag{8}$$

where S11 is the reflection coefficient of the arc antenna.

The radiation power density of arc antenna can be presented by the transmitted power and E-field as (7) and (8):

$$W = \frac{G_t}{4\pi R^2} P_t \tag{9}$$

$$W = \frac{E^2}{Z_0} \tag{10}$$

where G_t is the gain of antenna, Z_0 is the impedance of free space which is equal to 120π approximately, and R is the distance to the antenna.

With (8), (9) and (10), we can get

$$E = \sqrt{\frac{30 \cdot G_t \cdot \left(1 - |S11|^2\right)}{R^2}} \cdot \sqrt{P_{in}} \tag{11}$$

This article has been accepted for publication in a future issue of this journal, but has not been fully edited. Content may change prior to final publication. Citation information: DOI 10.1109/TVT.2017.2704611, IEEE Transactions on Vehicular Technology

At the same position, the value under the first square root is a constant, which means E-field is proportional to square root of P_{in}. Thus the real E-field of pantograph arcing along the railway can be calculated as (12).

$$E_{ARC} = E_{1W} \cdot \sqrt{P_{ARC} / 1W} \tag{12}$$

where E_{ARC} is the E-field generated by real pantograph arcing, and E_{1W} is the E-field calculated in numerical train models by 1W arc input power.

Fig. 22(a) shows the E_{ARC} along the line 0.1 height above the middle of train roof. Fig. 22(b) shows the E_{ARC} beside the train roof 0.6 right away. The results are valuable for arranging the positions of sensitive equipment by the susceptibility limit.

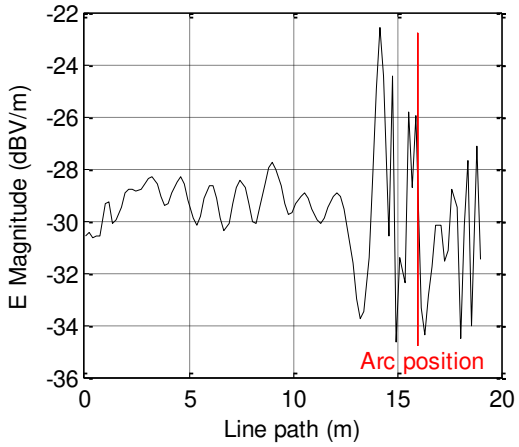

(a) The E-field on the line above the middle of train roof 0.1m height

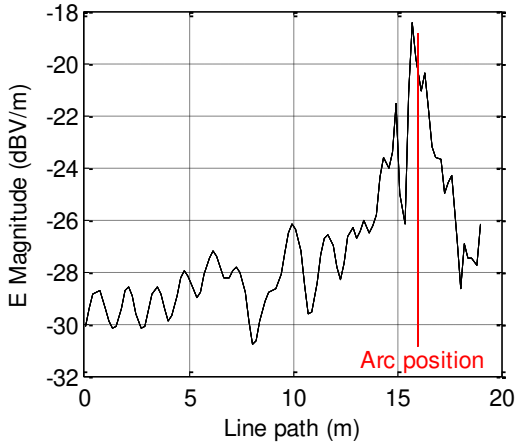

(b) The E-field on the line beside the train roof 0.6m right

Fig. 22. The E-field on the line with arc power at RBW 300kHz

C. *Application Scope and Limitation of the Method*

The method introduced in this paper is suitable to calculate the radiated coupling disturbance between pantograph arcing and sensitive system on board and the electromagnetic field beside the railway. The sensitive system should have at least one part performing as a receive antenna, which can be a real antenna, a cable, an aperture and any other structures which behave as an antenna.

The model to calculate the coupling coefficient by CONCEPT II in this paper only include the necessary structures for pantograph arcing and GSM-R antenna. When this method is used to other sensitive device, for instance, the device inside the train, the full carriage with windows and the "receive antenna" of the device should be built in the model. This will require a large computer memory and long calculation time.

The pantograph arcing replica made in this paper is a simple model used to present the measurement method of the radiated power of pantograph arcing. It will be more accurate to utilize 25kV/50Hz AC power supply and the same material of pantograph and contact wire used in railway to improve the replica. With the same DC motor, the line speed of the wheel edge (simulate the train speed) is limited by the wheel size. A larger wheel and a larger reverberation chamber can achieve results in higher speeds and lower frequencies.

V. CONCLUSION

A novel method for calculating the radiated coupling power from pantograph arcing in high-speed railway is proposed. By combing numerical simulation and laboratory measurements methods, the coupling power is calculated by the coupling coefficient and the total radiated power of arcing.

The coupling coefficient between pantograph arcing and the sensitive equipment is obtained by a series of numerical models. Meanwhile, the variability of the coupling coefficient is also considered by simulating four possible situations (inclined arcing, zigzag structure of contact wire, oscillation of contact wire or train and folding pantograph) during the train running.

The total radiated power of pantograph arcing is accomplished by measurements in the reverberation chamber with a speed-controllable pantograph arcing replica. Pulse signal has been proposed and verified to be a valid reference source when measuring the radiated power of arcing.

With the coupling coefficient and the total radiated power of arcing, the coupled power received by the sensitive equipment can be calculated. The electromagnetic field of pantograph arcing also can be calculated by the numerical model and the total radiated power.

This method can solve the problem in electromagnetic simulation that the source can't represent the real pantograph arcing in railway. Comparing to on-site measurement, this method uses a pantograph arcing replica which can fully control the train speed and other generating conditions of arcing to repeat the same experiment. The calculated results can be used to predict whether the radiation of pantograph arcing can interfere the train control system and is valuable for arranging the positions of sensitive equipment. In addition, more accurate results can be achieved by an improved replica and measurements in large reverberation chamber.

ACKNOWLEDGE

We thank York EMC Services for their support and assistance to build the laboratory replica of pantograph arcing.

REFERENCES

[1] Midya S, Bormann D, Mazloom Z, Schutte T, Thottappillil R, editors. Conducted and radiated emission from pantograph arcing in AC traction

system. Power & Energy Society General Meeting, 2009 PES'09 IEEE; 2009: IEEE.

[2] H. Fridhi, V. Deniau, J. P. Ghys, M. Heddebaut, J. Rodriguez, and I. Adin, "Analysis of the coupling path between transient EM interferences produced by the catenary-pantograph contact and on-board railway communication antennas," in *Proc. 2013 Int. Conf. on ICEAA*, Torino, 2013, pp.587-590.

[3] A. Mariscotti, A. Marrese, N. Pasquino, and R. Schiano Lo Moriello, "Time and frequency characterization of radiated disturbance in telecommunication bands due to pantograph arcing," *Meas. Journal*, vol. 46, pp. 4342-4352, 2013.

[4] A. Mariscotti and V. Denian, "On the characterization of pantograph arc transients on GSM-R antenna," in *17th IMEKO TC 4*, Kosice, 2010, pp.75-80.

[5] B. Tellini, M. Macucci, R. Giannetti, and G. A. Antonacci, "Conducted and radiated interference measurements in the line-pantograph system," *IEEE Trans. Instrum. Meas.*, vol. 50, no. 6, pp. 1661-1664, Dec. 2001.

[6] S. Midya, D. Bormann, T. Schutte, and R. Thottappillil, "Pantograph Arcing in Electrified Railways-Mechanism and Influence of Various Parameters-Part I: With DC Traction Power Supply," *IEEE Trans. Power Delivery*, vol. 24, no. 4, pp. 1931-1939, Oct. 2009.

[7] S. Midya, D. Bormann, T. Schutte, and R. Thottappillil, "Pantograph Arcing in Electrified Railways-Mechanism and Influence of Various Parameters-Part II: With AC Traction Power Supply," *IEEE Trans. Power Del.*, vol. 24, no. 4, pp. 1940-1950, Oct. 2009.

[8] S. Midya, D. Bormann, T. Schutte, and R. Thottappillil, "DC Component From Pantograph Arcing in AC Traction System-Influencing Parameters, Impact, and Mitigation Techniques," *IEEE Trans. Electromagn. Compat.*, vol. 53, no. 1, pp. 18-27, Feb. 2011.

[9] Das J, Mullick S K, Chatterjee P K. Principles of digital communication[M]. Cambridge University Press, 2008.

[10] Institute of EM Theory, Hamburg University of Technology. CONCEPT-II. (2013) [Online]. Available: http://www.tet.tuhh.de/downloads/concept/CONCEPT-II-September-2013.pdf

[11] Cassie A M. A new theory of arc rupture and circuit severity[C]//Conférence Internationale des Grands Réseaux Électriques à Haute Tension (CIGRE).–Paris. 1939: 1-14.

[12] Mayr O. Beiträge zur Theorie des statischen und des dynamischen Lichtbogens[J]. Archiv für Elektrotechnik, 1943, 37(12): 588-608.

[13] Sinclair G. Theory of Models of Electromagnetic Systems[J]. Proceedings of the Ire, 1948, 36(11):1364-1370.

[14] L. Ma, A. Marvin, Y. Wen, E. Karadimou and R. Armstrong, "An Experimental Programme to Determine the Feasibility of Using a Reverberation Chamber to Measure the Total Power Radiated by an Arcing Pantograph," in *Proc. 2014 Int. Sym. EMC Europe*, Gothenburg, 2014, pp.269-273.

[15] Int. Elect. Commission, 61000-4-21 Electromagnetic Compatibility (EMC), Part 4: Testing and Measurement Techniques, Section 21: Reverberation Chamber Test Methods.

Lan Ma (M'12) received her B.S. degree in Communication Engineering from Beijing Jiaotong University in 2010. She is currently pursuing the Ph.D. degree in Traffic Information Engineering and Control at EMC Laboratory, Beijing Jiaotong University.

She was a joint Ph.D. student at Department of Electronic Engineering, University of York, UK. Her research interests is electromagnetic interference in high-speed railway.

Yinghong Wen (M'01-SM'09) received her B.S., M.S., and Ph.D. degrees in Wireless Communication, Telecommunication and Information Engineering and Control from Beijing Jiaotong University in 1992, 1995 and 1998 respectively.

Since 1998 she has been on the faculty at School of Electronic and Information Engineering in Beijing Jiaotong University. She was a visiting scholar in University of Hawaii in 2008 and in University of York in 2015, and currently she is the Professor and Vice Dean of School of Electronic and Information Engineering in Beijing Jiaotong University. Her research interests include electromagnetic compatibility, antenna technology, radio waves propagation and transportation engineering.

Prof. Wen is a senior member of the Institute of Electrical and Electronic Engineers (IEEE) and Chinese Institute of Electronics. And she is also the secretary-general of IEEE China Council. She received an IEEE Member Recruitment and Recovery Committee Recognition for her outstanding achievement in member retention for Beijing Section during the 2015 membership year.

Andy Marvin (M'85–SM'06–F'11) received the B.Eng., M.Eng., and Ph.D. degrees from the University of Sheffield, Sheffield, South Yorkshire, U.K., between 1972 and 1978.

He is currently the Technical Director of York EMC Services Ltd. and a Professor of Applied Electromagnetics in the Communication Technologies Group, University of York's Department of Electronic Engineering, York, U.K.

Eva Karadimou received her B.S. degree in Electrical and Computer Engineering from National Technical University of Athens, Greece in 2011 and MSc by Research degree in Electronic Engineering from the University of York, U.K. in 2013.

She is currently an EMC Engineer working on Electromagnetic Compatibility aspects in York EMC Services Ltd since 2013.

Rob Armstrong received his B.Sc. degree (2007) and his MSc by Research (2009) in Physics at the University of York. Rob then studied for a PhD in the University of York's Department of Electronic Engineering, completed in 2013. He is currently Consultancy and Training Manager and Senior EMC Engineer with a specialism in Rail EMC at York EMC Services Ltd.

Hefei Cao received his B.S., M.S., and Ph.D. degrees from the Hebei Normal University in 2002, 1997 and 2012.

He is currently the Communication Engineering from Beijing Jiaotong University. His research interests is electromagnetic interference, electrostatic and electromagnetic shielding.